TISSUE ENGINEERING: Part A
Volume 21, Numbers 17 and 18, 2015
© Mary Ann Liebert, Inc.
DOI: 10.1089/ten.tea.2014.0572

termis
Tissue Engineering
& Regenerative Medicine
International Society

ORIGINAL ARTICLE

Extracellular Calcium Modulates Chondrogenic and Osteogenic Differentiation of Human Adipose-Derived Stem Cells: A Novel Approach for Osteochondral Tissue Engineering Using a Single Stem Cell Source

Liliana F. Mellor, PhD,[1] Mahsa Mohiti-Asli, PhD,[1] John Williams, MS,[1] Arthi Kannan, BS,[1] Morgan R. Dent, BS,[1] Farshid Guilak, PhD,[2] and Elizabeth G. Loboa, PhD[1,3]

We have previously shown that elevating extracellular calcium from a concentration of 1.8 to 8 mM accelerates and increases human adipose-derived stem cell (hASC) osteogenic differentiation and cell-mediated calcium accretion, even in the absence of any other soluble osteogenic factors in the culture medium. However, the effects of elevated calcium on hASC chondrogenic differentiation have not been reported. The goal of this study was to determine the effects of varied calcium concentrations on chondrogenic differentiation of hASC. We hypothesized that exposure to elevated extracellular calcium (8 mM concentration) in a chondrogenic differentiation medium (CDM) would inhibit chondrogenesis of hASC when compared to basal calcium (1.8 mM concentration) controls. We further hypothesized that a full osteochondral construct could be engineered by controlling local release of calcium to induce site-specific chondrogenesis and osteogenesis using only hASC as the cell source. Human ASC was cultured as micromass pellets in CDM containing transforming growth factor-β1 and bone morphogenetic protein 6 for 28 days at extracellular calcium concentrations of either 1.8 mM (basal) or 8 mM (elevated). Our findings indicated that elevated calcium induced osteogenesis and inhibited chondrogenesis in hASC. Based on these findings, stacked polylactic acid nanofibrous scaffolds containing either 0% or 20% tricalcium phosphate (TCP) nanoparticles were electrospun and tested for site-specific chondrogenesis and osteogenesis. Histological assays confirmed that human ASC differentiated locally to generate calcified tissue in layers containing 20% TCP, and cartilage in the layers with no TCP when cultured in CDM. This is the first study to report the effects of elevated calcium on chondrogenic differentiation of hASC, and to develop osteochondral nanofibrous scaffolds using a single cell source and controlled calcium release to induce site-specific differentiation. This approach holds great promise for osteochondral tissue engineering using a single cell source (hASC) and single scaffold.

Introduction

Calcium is a critical ion in cell biology that plays a key role in a number of cell functions necessary for cell homeostasis. Important cell functions are often directed by the transport of calcium (Ca^{2+}) across the cell membrane, into the cytoplasm from intracellular stores, or the allosteric binding of Ca^{2+} to a protein.[1,2] Calcium can act as a second messenger translating mechanical load to a chemical signal directing cell activity, as with certain stretch-activated mechanotransducers.[2–4] It can further act as a first messenger, binding with proteins outside of cell membranes, causing a cascade of signals within the cell.[5]

Elevated Ca^{2+} has been shown to affect cell differentiation in various cell types. It has been reported that increasing the extracellular Ca^{2+} levels from 0.03 to 1.2 mM leads to increased intracellular Ca^{2+} as well as the production of differentiation-related genes in keratinocytes.[6]

[1]Joint Department of Biomedical Engineering at University of North Carolina at Chapel Hill, North Carolina State University, Raleigh, North Carolina.
[2]Departments of Orthopedic Surgery and Biomedical Engineering, Duke University Medical Center, Durham, North Carolina.
[3]Department of Materials Science and Engineering, North Carolina State University, Raleigh, North Carolina.

Elevating extracellular Ca^{2+} to 2.5 mM has been shown effective in diminishing adipogenic differentiation, as evidenced by decreased cytoplasmic lipids, and downregulating the gene expression of adipogenic markers in 3T3-L1 preadipocytes.[7] It has also been reported that elevated Ca^{2+} is effective in directing osteogenic lineage specification of dental pulp cells. Ca^{2+} concentrations from 1.8 to 16.2 mM were analyzed, and it was found that higher concentrations increased matrix mineralization, without a significant impact on cell proliferation.[8]

We have previously reported the effects of three different calcium concentrations (1.8, 8, and 16 mM) on hASC osteogenesis for hASC in 2D monolayer culture maintained in a complete growth medium (CGM) or osteogenic differentiation medium,[9] and in electrospun scaffolds containing different concentrations of tricalcium phosphate (TCP).[10] We showed that exposure to 8 mM Ca^{2+} concentration resulted in the greatest hASC osteogenesis and cell-mediated calcium accretion; these effects were significantly decreased at 16 mM Ca^{2+} concentration. These findings are consistent with previous studies showing that ionic calcium levels between 6 and 10 mM significantly increased osteoblast mineralization, whereas concentrations above 10 mM can be cytotoxic.[11]

However, elevated Ca^{2+} has been found to be detrimental for chondrocyte growth and proliferation. Previous investigators have shown the impact of extracellular Ca^{2+} in chondrocyte death within damaged cartilage tissue.[12] For example, damaged cartilage that was cultured in Ca^{2+}-free medium showed significantly lower cell death after 2.5 h than tissue cultured in Ca^{2+}-rich media (2–20 mM). Increasing Ca^{2+} resulted in increased cell death, all within the superficial zone of the cartilage tissue. However, at day 7, greater cell death occurred in the deep zone of the cartilage tissue cultured in Ca^{2+}-free medium relative to samples cultured in Ca^{2+}-rich medium,[12] further demonstrating the effects of Ca^{2+} on cartilage tissue viability, and the varied response within different layers of articular cartilage to Ca^{2+} concentrations.

Human adipose-derived stem cells (hASC) provide an abundant and easily accessible source of cells for tissue engineering,[13] and previous studies have shown the ability of these cells to differentiate into osteogenic or chondrogenic lineages under appropriate culture conditions.[10,14,15] Our laboratory has previously published the effects of elevating Ca^{2+} levels on hASC osteogenesis, in both complete growth and osteogenic differentiation media, comparing mineralization and proliferation.[9,10,16] The use of elevated Ca^{2+} to direct hASC osteogenic lineage specification is a clear advantage in bone tissue engineering. However, the impact of elevated Ca^{2+} has not been widely studied in chondrogenic differentiation of hASC and cartilage tissue engineering. The ability to influence osteogenic or chondrogenic differentiation through modulation of extracellular Ca^{2+} may provide a novel means of inducing osteochondral regeneration using a single cell source and single scaffold.

Therefore, the purpose of this study was to determine the effects of elevated Ca^{2+} on combined osteogenic and chondrogenic differentiation of hASC. Our experimental approach was to compare chondrogenic factors in hASC treated with elevated (8 mM) or basal (1.8 mM) Ca^{2+} concentrations. We hypothesized that 8 mM Ca^{2+} would inhibit hASC chondrogenesis relative to 1.8 mM Ca^{2+} and induce a differentiation phenotype representing a combination of both hASC osteogenesis and chondrogenesis. We then used a similar approach to investigate the potential of using elevated Ca^{2+} to develop osteochondral constructs using a multilayer nanofibrous construct developed by our laboratory [10,17] capable of delivering varied Ca^{2+} concentrations. The multilayered construct was composed of electrospun polylactic acid (PLA) nanofibrous scaffolds bound together through polymerization of type I collagen gel.[11]

For this study, we developed a five-layer scaffold composed of three pure PLA nanofibrous layers within the upper region where cartilage generation was desired and two layers containing 20 wt% TCP nanoparticles within the bottom region where bone generation was desired. We have previously shown that these TCP/PLA composite nanofibers will release Ca^{2+} and promote the osteogenic differentiation of hASCs.[10,16] We hypothesized that the five-layer scaffolds composed of two distinct but integrated layers of nanofibers would promote site-specific hASC chondrogenic and osteogenic differentiation to create cartilaginous and bone-like tissues in one construct.

Although previous studies have used a single stem cell source to develop osteochondral tissue,[18–26] the approaches usually involve local delivery of growth factors through microspheres to the different layers,[19] or complex fabrication of multiphasic scaffolds using different materials or composites to resemble the different architectures of the native osteochondral tissue,[18,22,23] or used a combination of osteogenic (beta-glycerophosphate) and chondrogenic (insulin) factors within the scaffold,[24] complex double-chamber bioreactors,[25,27] or complex integrated scaffolds.[26] Graded TCP electrospun scaffolds have also been used with mouse preosteoblast cells (MC3T3-E1) to induce continuous mineralized tissue representative of the bone–cartilage interface, but not cartilage tissue.[28] Our study uses a simple calcium gradient scaffold approach to simultaneously modulate both osteogenesis and chondrogenesis of human adipose-derived stem cells without the need of bioreactors or different types of media. This approach is novel and provides a facile and translatable approach for osteochondral tissue engineering using abundant and accessible adipose-derived stem cells.

Materials and Methods

Isolation and culture of hASC

Excess adipose tissue was obtained from five premenopausal donors (24- to 36-year-old females, three Caucasian, one Native American, and one of unknown ethnicity) in accordance with an approved IRB protocol at UNC Chapel Hill (IRB 04-1622) and as described previously by our laboratory.[15] Human ASCs were isolated from the tissue using a method described previously by our laboratory and others.[9,10,14,15,29–33] At second passage, 100,000 cells of each cell line were seeded in a single T-75 flask in CGM comprised of alpha-modified minimal essential medium (α-MEM with L-glutamine; Invitrogen, Carlsbad, CA) supplemented with 10% fetal bovine serum (FBS, Premium Select; Atlanta Biologicals, Lawrenceville GA), 200 mM L-glutamine, and 100 IU penicillin/100 μg/mL streptomycin (Mediatech, Herndon, VA). The cells were allowed to proliferate at 37°C in 5% carbon dioxide until reaching 80% confluency, and

then passaged. The amassed cells were then characterized for osteogenic and adipogenic potential, ensuring that the cells differentiated representative of an average of the five cell lines.[15]

Pellet culture

After the third passage, hASCs were resuspended at a density of 250,000 cells per pellet. Cells were centrifuged at 300 *g* for 5 min to allow a pellet to form at the bottom of the tube. Pellets were cultured in 1 mL of selected chondrogenic differentiation medium (CDM) at either basal levels of Ca^{2+} (1.8 mM) or elevated Ca^{2+} (8 mM) concentration.[9] Calcium concentration was elevated by dissolving $CaCl_2$ (Sigma, St. Louis, MO) in the culture medium. Chondrogenic differentiation media were changed every 48 h by removing 0.5 mL of the media and replacing with fresh media.

Characterization of chondrogenic medium

Pellets were cultured in one of six CDM formulations (Table 1). All six chondrogenic media were primarily comprised of Dulbecco's modified Eagle's medium (Mediatech), 1% dexamethasone (Sigma), 1% ITS+ (Sigma), 1% Pen/Strep, and 1% ascorbic acid (Sigma), with varying combinations of FBS, bone morphogenetic protein 6 (BMP6), and transforming growth factor β1 (TGF-β1), as outlined in Table 1. Pellets were cultured at 37°C in 5% carbon dioxide for 28 days, receiving conditioned media changes every 48 h, by removing and replacing half of the media to preserve growth factors secreted by the cells. Ascorbic acid and chondrogenic growth factors, TGF-β1 and BMP6, were added to each medium formulation immediately before conditioned media changes. Cell pellets were then dehydrated, paraffin embedded, and sectioned for histological analyses. Sections were stained with Alcian blue (Sigma) to analyze glycosaminoglycan (GAG) content, as well as immunohistochemical (IHC) staining for *collagen type II*. IHC was conducted with a Histostain-Plus Kit (Invitrogen) utilizing primary antibodies for *collagen type II* (II-II6B; DSHB, IOWA city, IA). Pellet cultures grown under different differentiation media from Table 1 were evaluated.

Table 1. Chondrogenic Differentiation Media Formulations

Formulation No.	*Components*
1	No FBS
2	No FBS, TGF-β1 (10 ng/mL)
3	No FBS, TGF-β1 (10 ng/mL), BMP6 (10 ng/mL)
4	10% FBS
5	10% FBS, TGF-β1 (10 ng/mL)
6	10% FBS, TGF-β1 (10 ng/mL), BMP6 (10 ng/mL)

Six different media conditions were evaluated to optimize pellet growth conditions. All formulations were comprised of Dulbecco's modified Eagle's medium, 1% dexamethasone, 1% ITS+, 1% Pen/Strep, and 1% ascorbic acid. Only FBS and chondrogenic factors TGF-β1 and BMP6 varied among formulations.

BMP6, bone morphogenetic protein 6; FBS, fetal bovine serum; TGF-β1, transforming growth factor-β1.

Real-time reverse transcriptase–polymerase chain reaction analyses

Pellets from each condition were collected after 28 days of culture for quantitative reverse transcriptase–polymerase chain reaction (RT-PCR) analyses. Total RNA from three pellets per condition were homogenized and resuspended in TRIzol reagent (Invitrogen) following the manufacturer's instructions. The mRNA concentration and purity were determined using a NanoDrop spectrophotometer (Thermo Scientific, Wilmington, DE). The RNA was reverse-transcribed using SuperScript III First-Strand Synthesis System for qRT-PCR with oligo (dT) primers kit (Invitrogen) and amplified using an ABI Prism 7000 system (Applied Biosystems, Carlsbad, CA). The amplified PCR product was detected using SYBR Green reagents (Life Technologies, Grand Island, NY), with primer-specific amplification performed at 60°C for 30 s, and fluorescent quantification performed at 72°C. Each analysis was performed in triplicate. The following primers were designed using the Integrated DNA Technologies website: *Aggrecan forward* 5′-CAGGCAGATCACTTGAGGTTAG-3′ *reverse* 5′-CTC CCTAGTAGCTGGGATTACA-3′; *collagen I forward* 5′-AGAGTGGAGCAGTGGTTACTA-3′ *reverse 5′*-GATAC AGGTTTCGCCAGTAGAG-3′; *collagen II forward* 5′-TG GCCCTCAAGGATTTCAAG-3′ *reverse* 5′-ACCATCATC ACCAGGCTTTC-3′; *Runx2 forward* 5′-CATCACTGTC CTTTGGGAGTAG-3′ *reverse* 5′-ATGTCAAAGGCTGT CTGTAGG-3′; *β-actin forward* 5′-CACTCTTCCAGCCT TCCTTC-3′ *reverse* 5′-GTACAGGTCTTTGCGGATGT-3′. Signals were normalized to β-actin expression levels using the $-\Delta\Delta CT$ method.[34]

Statistical analyses

Statistical analyses were performed using IBM SPSS software (version 22; IBM, Armonk, NY). A paired *t*-test for each gene was performed to determine the statistical significance between the two groups. *p*-Values below 0.05 were considered statistically significant.

Fabrication of nanofibrous scaffolds

Biodegradable, biocompatible PLA (molecular weight of 70,000 g/mol) was dissolved in chloroform and dimethylformamide (Sigma) at a ratio of 3:1 to create a 12% solution. The solution was mixed continuously at 80°C for 12 h. The PLA solution was electrospun immediately after preparation at a feed rate of 0.7 μL/h using 15 kV, and regular single-component nanofibrous scaffolds were collected on a static collector spaced about 15 cm from the tip of the needle. Scaffolds were cut into squares of 1×1 cm^2. The nanofibrous scaffolds were then needle-punched (30 pores/layer) to create micron-sized pores with a pore diameter of 300 μm.

Construction of stacked scaffolds

PLA scaffolds were sterilized in 70% ethanol for 10 min and rinsed with phosphate-buffered saline three times before culturing cells on the scaffolds. Scaffolds were then placed in 24-well plates and soaked in CGM for 12 h. Human ASC (passage 3) were seeded at 250,000 cells/cm^2 on PLA nanofibers with 0% TCP and 20,000 cells/cm^2 on 20% TCP-loaded nanofibers, then cultured in 100 μL of CGM. After

hASC-seeded nanofibrous scaffolds were incubated for 3 h to allow cells to adhere, the five layers were then stacked together using type I collagen gel at a concentration of 3 mg/mL (Vitrogen; Angiotech BioMaterials Corporation, Palo Alto, CA).[10] Collagen I was first neutralized to pH 7.0 with 1 N NaOH, and 100 mL pipetted between the layers. The stacked constructs were incubated for 2 h to allow the collagen gel to polymerize, and then transferred to new 24-well plates with 1 mL culture medium. The constructs were cultured for 7 days in CGM, with medium changes every 3 days. After 7 days, CGM was replaced with CDM and scaffolds remained in this medium for the remaining 3 weeks, with conditioned medium change every 3 days, for a total culture time of 28 days.

Histological analyses

After 28 days in culture, pellets from elevated 8 mM Ca^{2+} conditions, pellets from basal 1.8 mM Ca^{2+} conditions, and stacked scaffolds were collected for histological analyses. Samples were fixed in 10% buffered formalin for 24 h, dehydrated with a graded series of ethanol, embedded in paraffin blocks, and sectioned in 10 μm (pellets) or 6 μm (stacked scaffolds)-thick slices. Sections were stained with Safranin O (Thermo Fisher, Waltham, MA) or Alcian blue to assess GAG content, and with Alizarin red to evaluate cell-mediated calcium accretion. Histochemical staining for collagen expression was conducted using primary antibodies for *collagen II* (Abcam #3092, Cambridge, UK), *collagen I* (Abcam #90395), and *collagen X* (Sigma #c7974) and a horseradish peroxidase detection system (DAB Substrate Kit; Vector Laboratories, Burlingmae, CA) following the manufacturer's instructions. *Collagen I* immunohistochemistry was performed using a primary *collagen I* antibody (1:100 dilution; Abcam #90395) followed by an Alexa Fluor 488 goat anti-mouse IgG (1:200 dilution; Life Technologies, Carlsbad, CA) secondary antibody. Images were captured using a Leica EZ4 D Digital Steremicroscope (Leica Microsystems, Inc., Buffalo Grove, IL) equipped with a 40× water immersion, high-resolution camera (Hamamatsu, Hamamatsu, Japan), and SimplePCI image capture and analysis software (Compix, Sewickley, PA).

Scanning electron microscopy analysis

Field emission scanning electron microscopy (FESEM JEOL 6400 F) was used to characterize the surface morphology and microstructure of the ultrafine electrospun fibers at 15 kV accelerating voltage.

Results

Optimization of chondrogenic differentiation media

To optimize hASC chondrogenic differentiation, pellets were grown in six different formulations of CDM (Table 1), and analyzed for sulfated GAG content and collagen II expression. Pellets grown in the absence of 10% FBS, 10 ng/mL of BMP6, and 10 ng/mL of TGF-β1 (formulation 1) were negative for collagen II and GAG expression, and were unable to form a solid pellet. Similarly, pellets grown in TGF-β1 but no FBS or BMP6 (formulation 2) did not form a compact pellet, but showed light expression of GAGs toward the center of the forming pellet. Pellets grown in both chondrogenic growth factors without FBS (formulation 3) exhibited a solid center, but loose periphery along the pellet, and very low GAG and *collagen II* expression. Pellets grown with FBS but in the absence of both chondrogenic factors (formulation 4) were able to form a round and solid pellet, but showed scattered GAG and *collagen II* expression. Pellets grown in FBS and TGF-β1 but no BMP6 (formulation 5), exhibited a solid and round pellet morphology, but less GAG and *collagen II* expression when compared to CDM containing FBS and both chondrogenic factors (formulation 6, data not shown).

Our results indicated that the presence of FBS in the media was crucial for the formation of a round and compact pellet, and that both TGF-β1 and BMP6 were necessary for improved chondrogenic differentiation, as expected.[35] Based on this data, formulation 6 was chosen for all further experiments.

Immunohistological analyses of pellets cultured in varied calcium conditions

Human ASC pellets cultured in the same CDM but varied Ca^{2+} concentrations underwent dissimilar differentiation pathways. Morphologically, pellets cultured in the basal Ca^{2+} concentration (1.8 mM) formed round and compact pellets when compared to pellets cultured in elevated Ca^{2+} (8 mM) conditions. The outer peripheries of pellets cultured in 8 mM Ca^{2+} appeared stratified and loose, whereas control pellets cultured in basal 1.8 mM Ca^{2+} were uniformly dense and compact (Fig. 1). Additionally, pellets cultured in elevated Ca^{2+} conditions (8 mM) exhibited significant tissue mineralization as assessed by positive Alizarin red staining (Fig. 1B). After 28 days of culture in CDM, pellets grown in elevated Ca^{2+} (8 mM) mineralized, with more pronounced mineralization in the outer periphery, in closer proximity to the elevated Ca^{2+} in the medium. In contrast, pellets cultured in basal Ca^{2+} conditions (1.8 mM) were negative for Alizarin red staining and only showed fast green counterstain (Fig. 1A).

GAG content was also greater in pellets cultured in basal Ca^{2+} conditions (1.8 mM) suggesting greater chondrogenic differentiation when compared to pellets cultured with the same CDM, but at elevated Ca^{2+} concentration (8 mM) as assessed by Safranin O and Alcian blue stains (Fig. 1C–H). Higher magnification of the center of the pellets stained with Alcian blue indicate that hASC pellets cultured in 1.8 mM Ca^{2+} concentration exhibit a more chondrocyte-like phenotype (cells with lacunae) as compared to the more osteoblast-like phenotype for hASC cultured in elevated 8 mM Ca^{2+} conditions (Fig. 1G, H).

IHC analyses indicated that hASC cultured in 8 mM Ca^{2+} exhibited greater *collagen type I* and *X* expressions and less collagen type II expression than control hASC cultured in 1.8 mM Ca^{2+} (Fig. 2). Negative control pellets were obtained performing DAB (3,3′-diaminobenzidine) staining in the absence of a primary antibody (Fig. 2A, B). Location of collagen expression also varied within the experimental and control hASC pellets. In the 8 mM Ca^{2+} pellets, positive staining for collagen type I was more prevalent in the loose outer periphery of the pellets, whereas positive staining within the basal calcium pellets was more uniform throughout the pellet, with the exception of some negative staining

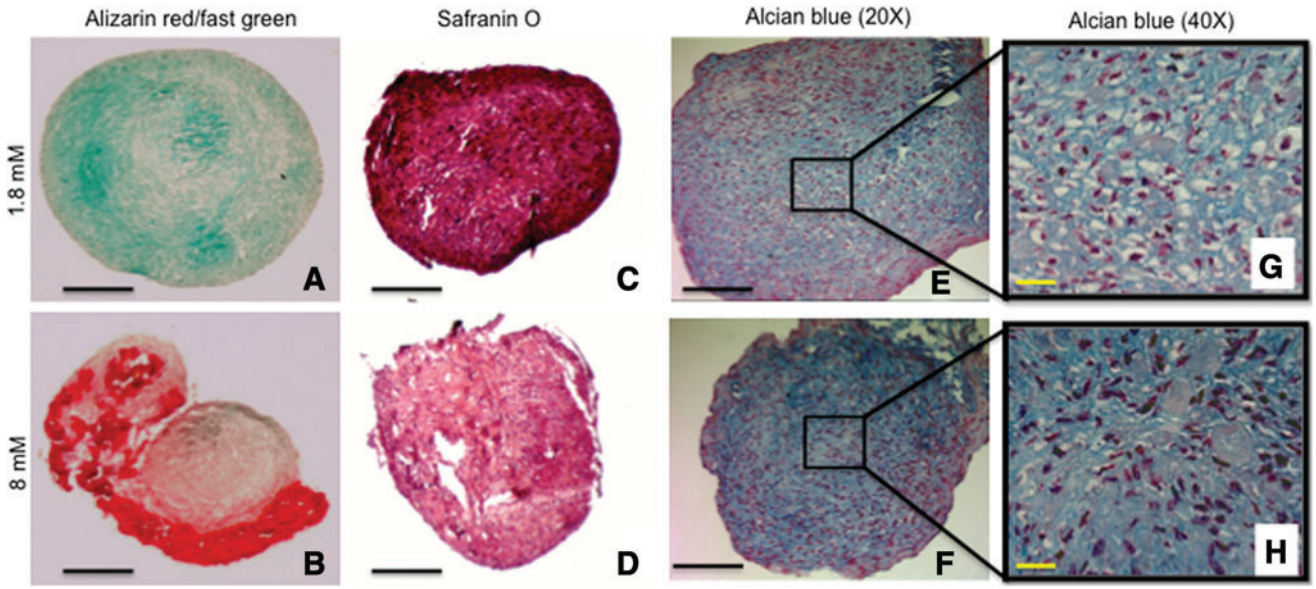

FIG. 1. Changes in tissue mineralization and glycosaminoglycan (GAG) production in response to different calcium concentrations. **(A, B)** Alizarin red staining (fast green counterstain) of pellet cultures of human adipose-derived stem cells cultured in chondrogenic differentiation medium (CDM) and elevated calcium (8 mM) shows excess tissue mineralization **(B)**, most notable in the outer periphery of pellet when compared to basal calcium (1.8 mM) conditions **(A)**. **(C, D)** Safranin O staining of pellet cultures in basal calcium (1.8 mM) shows increased GAG production **(C)** when compared to elevated calcium (8 mM) concentrations **(D)**. **(E, F)** Alcian blue/Hematoxylin staining of pellet cultures in basal calcium (1.8 mM) **(E)** and elevated calcium (8 mM) is similar, but closer view of the pellets shows that cells in 1.8 mM calcium have a more chondrocyte-like morphology **(G)** when compared to the 8 mM cells showing a more fibroblast-like morphology **(H)** (*Black scale bars* = 100 μm; *yellow scale bars* = 25 μm). Color images available online at www.liebertpub.com/tea

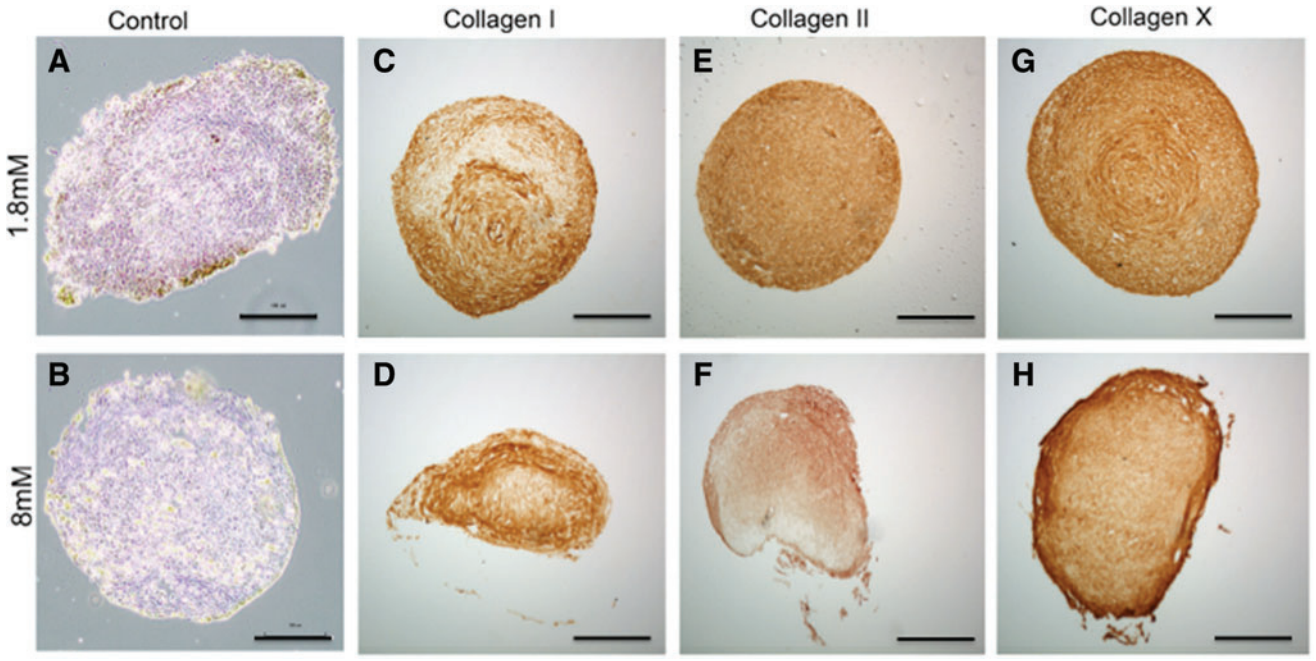

FIG. 2. Immunohistochemistry of human adipose-derived stem cell pellets cultured under different calcium concentrations. Pellets grown in CDM containing transforming growth factor-β1 (TGF-β1) and bone morphogenetic protein 6 (BMP6) at basal (1.8 mM) or elevated (8 mM) calcium concentrations were stained for **(C, D)** *collagen I*, **(E, F)** *collagen II*, and **(G, H)** *collagen X*. **(A, B)** Control pellets with no primary antibody and (scale bar = 100 μm). Color images available online at www.liebertpub.com/tea

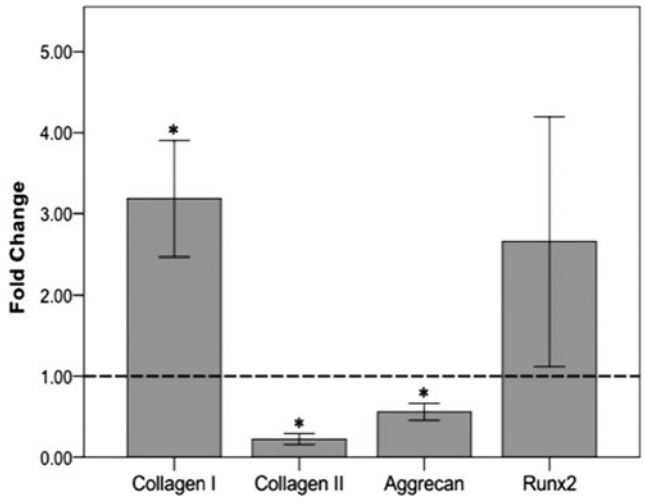

FIG. 3. Changes in gene expression of hASC pellets cultured in elevated calcium relative to pellets cultured in basal calcium conditions. Pellets grown in CDM containing TGF-β1 and BMP6 at elevated (8 mM) calcium concentrations exhibited increased *collagen I* and *Runx2* mRNA expression, and decreased *collagen II* and aggrecan mRNA expression relative to those cultured in basal calcium (1.8 mM) conditions (*dashed line*) as assessed by quantitative reverse transcriptase–polymerase chain reaction. All data were normalized to *β-actin* (*p-value < 0.05).

toward the middle of the pellet (Fig. 2C, D). Control 1.8 mM Ca^{2+} pellets also exhibited greater collagen type II expression relative to pellets cultured in elevated Ca^{2+} (8 mM) conditions (Fig. 2E, F). Although both 1.8 and 8 mM Ca^{2+} pellets exhibited positive staining for collagen type X within the center of each section, elevated Ca^{2+} (8 mM) pellets had stronger *collagen type X* staining in the loose outer periphery relative to the controls, suggesting a possible zone of hypertrophy in elevated Ca^{2+} conditions (Fig. 2G, H).

Changes in gene expression in pellets cultured under different calcium concentrations

To further assess hASC differentiation in pellets cultured in CDM at different Ca^{2+} concentrations, gene expression was analyzed in both conditions. Consistent with the histological findings, pellets cultured in elevated Ca^{2+} (8 mM) exhibited a significant increase in *collagen I* ($p = 0.038$) and *Runx2* ($p = 0.136$), and decreased synthesis of *collagen II* ($p = 0.0003$) and *aggrecan* mRNA expression ($p = 0.013$) when compared to the basal calcium (1.8 mM) control cells (Fig. 3).

Analyses of osteochondral constructs

SEM analyses confirmed that electrospun nanofibers were successfully loaded with TCP nanoparticles. Surface morphology analyses of the fibers confirmed the presence of TCP in the nanofibers (Fig. 4). The PLA electrospun layers were then stacked using two layers of 20% TCP-PLA scaffolds and three layers of 0% TCP-PLA scaffolds to generate a representative osteochondral scaffold (Fig. 5A, D**).** The electrospun layers were needle-punched before stacking to allow cell infiltration throughout the layers after the complete, stacked construct was created (Fig. 5B, C). To inhibit released TCP from the bottom layers affecting cells residing in the 0% TCP layers, media were changed every other day. This approach, in combination with the known precipitation of calcium downward (due to gravity) as opposed to upward, appeared successful.

Specifically, consistent with our hypothesis and pellet data, hASC differentiated in a site-specific manner in response to TCP concentrations to generate bone in the bottom

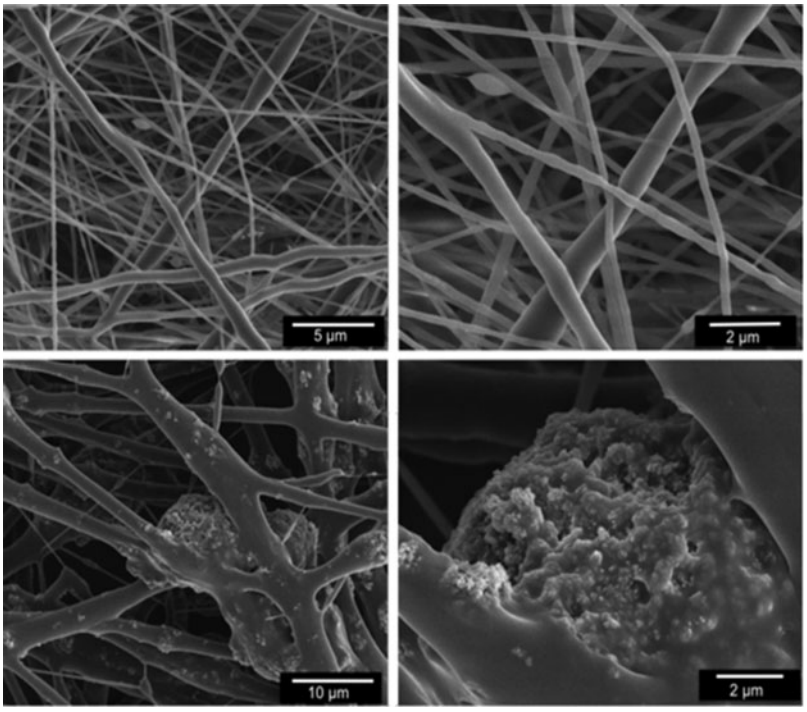

FIG. 4. Scanning electron microscopy of electrospun polylactic acid (PLA) fibers used to seed human adipose-derived stem cells. *Top panel* shows pure PLA fibers (0% tricalcium phosphate [TCP]) and *bottom panel* shows PLA fibers containing 20% TCP concentration.

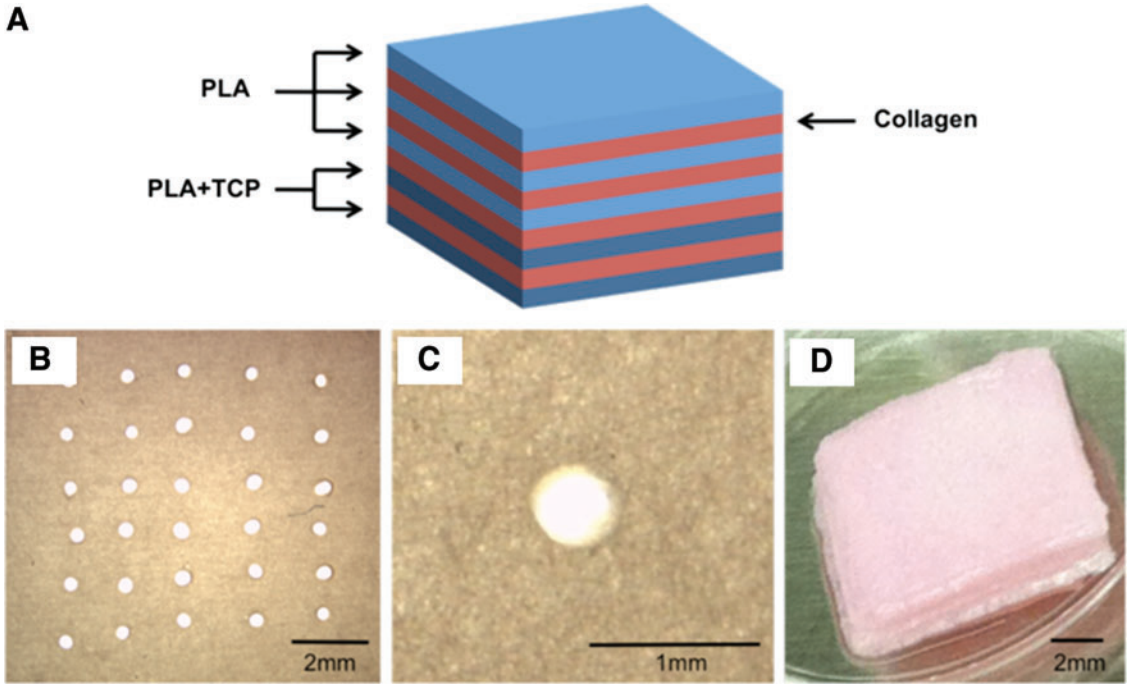

FIG. 5. Construction of stacked osteochondral constructs. **(A)** Schematic image of different layers in stacked osteochondral construct showing how the electrospun PLA nanofibers (*blue layers*) were stacked together using collagen I gel (*red layers*) in between nanofibrous layers to form the stacked construct. The *top* three layers were pure PLA (0% TCP) to allow chondrogenesis, and the *bottom* two layers contained 20% TCP to inhibit chondrogenesis and induce osteogenesis. **(B, C)** Light microscopy images of nanofibers with needle-punched pores; **(D)** image of a stacked construct containing three layers of pure PLA fibers and two layers 20% TCP-PLA fibers. Color images available online at www.liebertpub.com/tea

layers (20% TCP) and cartilage in the top layers (0% TCP) when cultured for 1 week in CGM followed by culture for 3 weeks in CDM containing TGF-β1 and BMP-6. Hematoxylin and eosin staining shows successful cell migration throughout the needle-punched nanofibrous PLA layers (Fig. 6A). Alizarin red staining of the stacked scaffold shows increased tissue mineralization in the bottom layers containing 20% TCP when compared to the superficial layers (Fig. 6B). Alcian blue staining shows increased chondrogenesis in the 0% TCP superficial layers when compared to the deep 20% TCP layers (Fig. 6C). Immunofluorescence of collagen I staining shows increased collagen I expression in the bottom layers containing 20% TCP when compared to the superficial layers with no TCP (Fig. 6D).

Discussion

The goal of this study was to investigate the effects of extracellular Ca^{2+} concentration on hASC chondrogenesis and the potential to use controlled Ca^{2+} delivery to induce site-specific chondrogenesis and osteogenesis using hASC seeded in a single scaffold. Our results supported our hypothesis that elevated Ca^{2+} inhibits hASC chondrogenesis and induces a differentiation phenotype representing a combination of both hASC osteogenesis and chondrogenesis, when cultured in optimal chondrogenic differentiation conditions. Histological analyses demonstrated clear differences between pellets cultured in basal 1.8 mM and elevated 8 mM Ca^{2+} concentrations, most notably in tissue mineralization and changes in *collagen I, II, and X* expressions. Morphologically, hASC pellets cultured in 8 mM Ca^{2+} exhibited loose and stratified layers toward the outer periphery of the pellet, as opposed to the round and compact uniform morphology of control pellets. Immunohistochemistry results for *collagen X* expression indicated enhanced *collagen X* staining within the loose peripheral layers of the elevated Ca^{2+} pellets.

Collagen X is associated with chondrocyte hypertrophy and ossification as well as calcified cartilage, where bone and cartilage tissue interact. These results suggest that cells in the outside of the pellet may have become hypertrophic and possibly undergoing endochondral ossification. This is consistent with previous studies showing the role of PTHrP in inhibiting hypertrophy in chondrocytes.[36–39] Parathyroid hormone-related protein is downregulated in environments of high Ca^{2+} concentration due to signaling through the extracellular calcium sensing receptor.[5,37] Increased PTHrP has been associated with increased chondrocyte proliferation and maintenance of cells in a matrix-forming phenotype, resulting in increased matrix production.[36,37]

Histological findings also demonstrated that both 8 and 1.8 mM Ca^{2+} pellets differentiated down the chondrogenic lineage, but to varying degrees. Safranin-O staining showed both conditions stained positive for sulfated GAGs, but pellets cultured in 1.8 mM Ca^{2+} exhibited greater positive staining than pellets cultured in 8 mM Ca^{2+}. These qualitative findings were further supported by changes in gene expression as assessed by quantitative RT-PCR analyses. After 28 days in culture, pellets in 8 mM Ca^{2+} expressed significant increases in *collagen I*, and decreased *collagen II* and *aggrecan* expression when compared to pellets cultured in 1.8 mM Ca^{2+}, suggesting that elevated 8 mM Ca^{2+}

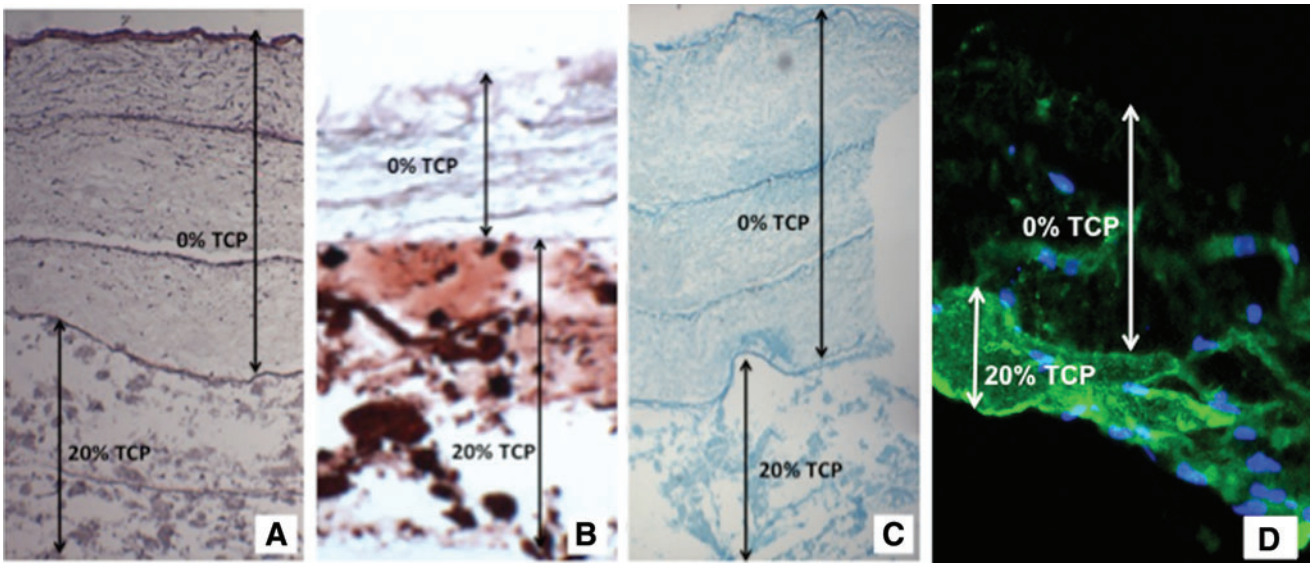

FIG. 6. Histochemical staining of stacked PLA scaffolds containing 0% or 20% TCP seeded with human adipose-derived stem cells (hASC) for 28 days. **(A)** Hematoxylin and eosin staining showing cells growing in all layers. *Dark lines* between stacks show regions of highest cell density where hASC were seeded on nanofibrous PLA or PLA/TCP scaffolds before stacking within collagen gel. **(B)** Alizarin red staining showing calcium accretion (*red*) in the 20% TCP-loaded nanofibers and none in 0% TCP-loaded nanofibers. **(C)** Alcian blue staining showing increased hASC chondrogenesis in *top* three layers (0% TCP). **(D)** Immunofluorescence for *collagen I* shows increased expression in the *bottom* 20% TCP layers when compared to the superficial 0% layers. Color images available online at www.liebertpub.com/tea

induced osteogenesis, regardless of the optimal culture conditions to induce chondrogenesis.

In addition to the histological and IHC analyses for chondrogenic markers, further analyses were performed to determine the effects of elevated 8 mM Ca^{2+} on osteogenic differentiation of hASC cultured in CDM. Pellets in 8 mM Ca^{2+} exhibited positive Alizarin red staining throughout the pellet, but more pronounced in the outer periphery, which was in closer contact to the elevated Ca^{2+} in the media. In contrast, pellets cultured in basal Ca^{2+} (1.8 mM) conditions were all negative for Alizarin red staining. Immunohistochemistry for *collagen I* showed that both control and experimental pellets stained positively, but in different locations. In 8 mM Ca^{2+} sections, positive IHC staining was mostly localized to the loose outer layers of the pellet, whereas the 1.8 mM Ca^{2+} pellets demonstrated positive *collagen I* staining in a swirled pattern in the center of the pellet.

The mechanisms responsible for these positive results are not clear and require further study. However, we suspect that the calcium sensing receptor (CaSR) may play a role in inhibiting chondrogenesis in response to increased extracellular calcium, as it has been shown to be expressed and functionally active in osteoblast-like cell lines[40] and several types of stem cells, including human and ovine amniotic fluid stem cells,[41] equine umbilical cord matrix,[42] and bone marrow mesenchymal stem cells (MSCs).[43] More recently, the calcium-sensing receptor was reported to play a potential role in the osteogenic differentiation of human amniotic fluid MSCs.[44]

This study demonstrates that culturing hASC in CDM at elevated 8 mM Ca^{2+} concentration results in inhibited hASC chondrogenesis. While chondrogenic differentiation can occur to some extent, the cells in closest contact to the elevated Ca^{2+} environment, toward the outer portions of the pellet, appear to become hypertrophic, and possibly undergo endochondral ossification. Additionally, this process decreases the production of cartilage extracellular matrix components. These differences in cell morphology and extracellular matrix production may be indicative of varying mechanical properties within the pellet and this should be further studied. These data are promising for further osteochondral tissue engineering studies using hASC as a single cell source to produce both bone and articular cartilage by simply modulating Ca^{2+} concentrations.

As a first step on this path, we used a multilayered fabrication approach for local delivery of extracellular calcium to hASC to regulate site-specific osteogenesis and chondrogenesis. Generation of osteochondral tissue-engineered grafts requires an integrated combination of articular cartilage and bone tissue regeneration to mimic native osteochondral tissue.[45] Traditionally, chondrogenic and osteoblastic cell lines have been used as a source for osteochondral regeneration, but the limited supply and regenerative capabilities of primary cells can present a challenge for tissue regeneration. Therefore, the use of stem cells as an alternative resource is very promising.[46–48]

Although many investigators have successfully generated cartilage and bone tissue using stem cells, a remaining challenge is the generation of osteochondral tissue with cartilaginous and bone-like regions using a single stem cell source. Further, recreating the interphase between the cartilage and subchondral bone has been the most difficult challenge in successful osteochondral tissue engineering. This osteochondral junction consists of calcified cartilage, and has a critical mechanical and physiological role, acting as a biochemical barrier and mechanical transition between the soft cartilage and stiff subchondral bone.[49] Therefore,

such scaffolds must consist of a gradient or differential release of cytokines and/or growth factors to induce site-specific differentiation.

A popular approach for developing successful osteochondral tissue is using biphasic constructs, designed to induce bone formation in the deep layer and cartilage in the top layer.[50] Some researchers have attempted to develop barriers between the two layers to prevent infiltration of blood vessels into the cartilage tissue.[51,52] Although separation of the cartilage and bone tissues may be achieved, the mechanical properties of the two phases and integration of the two scaffolds into one construct present significant challenges, and lack a transitional zone between the two phases. A more recent approach to develop a full osteochondral construct used a dual growth factor delivery approach, for a spatially guided formation of osteochondral tissue.[53] Although most of these studies have successfully formed bone, cartilage, or both, the transitional interphase between the cartilage and subchondral bone that mimics both mechanically and biochemically the interphase of osteochondral tissue, remains a challenge.

Our technique of layering multiple nanofibrous scaffolds that differentially release extracellular calcium to induce hASC site-specific chondrogenesis and osteogenesis holds great potential for developing a full osteochondral construct. Nanofibers have morphological similarities to collagen nanofibers within the extracellular matrix of native tissue. Collagen nanofibers play an important role in maintaining the structural integrity of various tissues, including bone and cartilage.[54] We have previously shown that hASC attach and proliferate well on PLA nanofibers.[10,16,17] We also have extensive experience with incorporating TCP nanoparticles, an osteoconductive drug, in nanofibers and assessing their release profile and subsequent effect on hASC differentiation.[10,16]

According to our previous results, electrospun single component PLA nanofibers containing 20% TCP have a burst release profile releasing about 50% of calcium ions in the first day followed by the gradual release of the remaining calcium in the following days up to 36 days.[16] Although incorporating TCP particles in the PLA nanofibers increases the fiber diameter, we have previously shown that the change in fiber diameter does not have a negative effect on cell viability or proliferation of hASC.[10] Our previous results confirmed that hASC cultured in CGM on 20% TCP in single component PLA nanofibers differentiate down an osteogenic pathway. In this study, hASC also underwent osteogenic differentiation, as confirmed by Alizarin red staining, in a combination of CGM and chondrogenic growth medium when cultured in the 20% TCP/PLA bottom layers of the osteochondral scaffolds to successfully form a subchondral bone region. Cells seeded on pure PLA (0% TCP) nanofibers differentiated down the chondrogenic pathway. This suggests that the release of calcium ions from nanofibers not only induces osteogenesis, but also inhibits chondrogenesis in the presence of CDM, consistent with our findings from the pellet studies.

Conclusions

Our study reports the effects of elevated calcium on hASC chondrogenesis, and shows that extracellular Ca^{2+} can induce osteogenesis of hASC, even when cultured in optimal chondrogenic differentiation conditions. Our results show that hASC is able to chondrogenically differentiate in basal calcium conditions (1.8 mM); however, chondrogenesis is inhibited to a significant degree in elevated 8 mM Ca^{2+} conditions as shown by decreased matrix production and increased mineralization of the tissue. The potential use of regulated calcium release in designing osteochondral constructs was evaluated by developing a multilayer stacked nanofibrous construct with regional incorporation of TCP nanoparticles. This technique enabled differentiation of both cartilage and bone tissue in one continuous construct using only hASC as a single cell source. Further investigation to determine the material properties of the resulting tissue and the possible underlying mechanism(s) that modulate hASC differentiation in response to calcium concentrations are being investigated.

Acknowledgments

The authors would like to thank Dr. Brad Estes, Dr. Frank Moutos, and Dr. Susan Bernacki for their technical expertise and assistance with this project. This work was supported, in part, by the National Space Biomedical Research Institute through NASA NCC9-58, NIH/NIBIB 1R03EB008790 (EGL), NSF/CBET 1133427 (EGL), NIH AR48182 (FG), and NIH AR48852 (FG).

Disclosure Statement

No competing financial interests exist.

References

1. McCleskey, E.W., Fox, A.P., Feldman, D., and Tsien, R.W. Different types of calcium channels. J Exp Biol **124,** 177, 1986.
2. Liu, B., Kim, T.J., and Wang, Y. Live cell imaging of mechanotransduction. J R Soc Interface **7(Suppl 3),** S365, 2010.
3. Wong, M., and Carter, D.R. Articular cartilage functional histomorphology and mechanobiology: a research perspective. Bone **33,** 1, 2003.
4. Guilak, F., Leddy, H.A., and Liedtke, W. Transient receptor potential vanilloid 4: the sixth sense of the musculoskeletal system? Ann N Y Acad Sci **1192,** 404, 2010.
5. Brown, E.M., Chattopadhyay, N., Vassilev, P.M., and Hebert, S.C. The calcium-sensing receptor (CaR) permits Ca^{2+} to function as a versatile extracellular first messenger. Recent Prog Horm Res **53,** 257, 1998; discussion 280.
6. Tu, C.L., Chang, W., and Bikle, D.D. The extracellular calcium-sensing receptor is required for calcium-induced differentiation in human keratinocytes. J Biol Chem **276,** 41079, 2001.
7. Jensen, B., Farach-Carson, M.C., Kenaley, E., and Akanbi, K.A. High extracellular calcium attenuates adipogenesis in 3T3-L1 preadipocytes. Exp Cell Res **301,** 280, 2004.
8. An, S., Gao, Y., Ling, J., Wei, X., and Xiao, Y. Calcium ions promote osteogenic differentiation and mineralization of human dental pulp cells: implications for pulp capping materials. J Mater Sci Mater Med **23,** 789, 2012.
9. McCullen, S.D., Zhan, J., Onorato, M.L., Bernacki, S.H., and Loboa, E.G. Effect of varied ionic calcium on human adipose-derived stem cell mineralization. Tissue Eng Part A **16,** 1971, 2010.

10. McCullen, S.D., Zhu, Y., Bernacki, S.H., Narayan, R.J., Pourdeyhimi, B., Gorga, R.E., and Loboa, E.G. Electrospun composite poly(L-lactic acid)/tricalcium phosphate scaffolds induce proliferation and osteogenic differentiation of human adipose-derived stem cells. Biomed Mater **4,** 035002, 2009.
11. Maeno, S., Niki, Y., Matsumoto, H., Morioka, H., Yatabe, T., Funayama, A., Toyama, Y., Taguchi, T., and Tanaka, J. The effect of calcium ion concentration on osteoblast viability, proliferation and differentiation in monolayer and 3D culture. Biomaterials **26,** 4847, 2005.
12. Amin, A.K., Huntley, J.S., Bush, P.G., Simpson, A.H., and Hall, A.C. Chondrocyte death in mechanically injured articular cartilage—the influence of extracellular calcium. J Orthop Res **27,** 778, 2009.
13. De Girolamo, L., Sartori, M.F., Arrigoni, E., Rimondini, L., Albisetti, W., Weinstein, R.L., and Brini, A.T. Human adipose-derived stem cells as future tools in tissue regeneration: osteogenic differentiation and cell-scaffold interaction. Int J Artif Organs **31,** 467, 2008.
14. Estes, B.T., Diekman, B.O., Gimble, J.M., and Guilak, F. Isolation of adipose-derived stem cells and their induction to a chondrogenic phenotype. Nat Protoc **5,** 1294, 2010.
15. Bodle, J.C., Teeter, S.D., Hluck, B.H., Hardin, J.W., Bernacki, S.H., and Loboa, E.G. (2014) Age-related effects on the potency of human adipose-derived stem cells: creation and evaluation of superlots and implications for musculoskeletal tissue engineering applications. Tissue Eng Part C Methods **20,** 972, 2014.
16. Asli, M.M., Pourdeyhimi, B., and Loboa, E.G. Release profiles of tricalcium phosphate nanoparticles from poly(L-lactic acid) electrospun scaffolds with single component, core-sheath, or porous fiber morphologies: effects on hASC viability and osteogenic differentiation. Macromol Biosci **12,** 893, 2012.
17. McCullen, S.D., Miller, P.R., Gittard, S.D., Gorga, R.E., Pourdeyhimi, B., Narayan, R.J., and Loboa, E.G. In situ collagen polymerization of layered cell-seeded electrospun scaffolds for bone tissue engineering applications. Tissue Eng Part C Methods **16,** 1095, 2010.
18. Gao, J., Dennis, J.E., Solchaga, L.A., Awadallah, A.S., Goldberg, V.M., and Caplan, A.I. Tissue-engineered fabrication of an osteochondral composite graft using rat bone marrow-derived mesenchymal stem cells. Tissue Eng **7,** 363, 2001.
19. Wang, X., Wenk, E., Zhang, X., Meinel, L., Vunjak-Novakovic, G., and Kaplan, D.L. Growth factor gradients via microsphere delivery in biopolymer scaffolds for osteochondral tissue engineering. J Control Release **134,** 81, 2009.
20. Im, G.I., and Lee, J.H. Repair of osteochondral defects with adipose stem cells and a dual growth factor-releasing scaffold in rabbits. J Biomed Mater Res B Appl Biomater **92,** 552, 2010.
21. Guo, X., Park, H., Young, S., Kretlow, J.D., van den Beucken, J.J., Baggett, L.S., Tabata, Y., Kasper, F.K., Mikos, A.G., and Jansen, J.A. Repair of osteochondral defects with biodegradable hydrogel composites encapsulating marrow mesenchymal stem cells in a rabbit model. Acta Biomater **6,** 39, 2010.
22. Grayson, W.L., Bhumiratana, S., Grace Chao, P.H., Hung, C.T., and Vunjak-Novakovic, G. Spatial regulation of human mesenchymal stem cell differentiation in engineered osteochondral constructs: effects of pre-differentiation, soluble factors and medium perfusion. Osteoarthritis Cartilage **18,** 714, 2010.
23. Da, H., Jia, S.J., Meng, G.L., Cheng, J.H., Zhou, W., Xiong, Z., Mu, Y.J., and Liu, J. The impact of compact layer in biphasic scaffold on osteochondral tissue engineering. PLoS One **8,** e54838, 2013.
24. Erisken, C., Kalyon, D.M., Wang, H., Ornek-Ballanco, C., and Xu, J. Osteochondral tissue formation through adipose-derived stromal cell differentiation on biomimetic polycaprolactone nanofibrous scaffolds with graded insulin and Beta-glycerophosphate concentrations. Tissue Eng Part A **17,** 1239, 2011.
25. Liu, X.G., and Jiang, H.K. Preparation of an osteochondral composite with mesenchymal stem cells as the single-cell source in a double-chamber bioreactor. Biotechnol Lett **35,** 1645, 2013.
26. Ding, X., Zhu, M., Xu, B., Zhang, J., Zhao, Y., Ji, S., Wang, L., Wang, L., Li, X., Kong, D., Ma, X., and Yang, Q. Integrated trilayered silk fibroin scaffold for osteochondral differentiation of adipose-derived stem cells. ACS Appl Mater Interfaces **6,** 16696, 2014.
27. Mahmoudifar, N., and Doran, P.M. Osteogenic differentiation and osteochondral tissue engineering using human adipose-derived stem cells. Biotechnol Prog **29,** 176, 2013.
28. Erisken, C., Kalyon, D.M., and Wang, H. Functionally graded electrospun polycaprolactone and beta-tricalcium phosphate nanocomposites for tissue engineering applications. Biomaterials **29,** 4065, 2008.
29. Zuk, P.A., Zhu, M., Mizuno, H., Huang, J., Futrell, J.W., Katz, A.J., Benhaim, P., Lorenz, H.P., and Hedrick, M.H. Multilineage cells from human adipose tissue: implications for cell-based therapies. Tissue Eng **7,** 211, 2001.
30. McCullen, S.D., Stevens, D.R., Roberts, W.A., Clarke, L.I., Bernacki, S.H., Gorga, R.E., and Loboa, E.G. Characterization of electrospun nanocomposite scaffolds and biocompatibility with adipose-derived human mesenchymal stem cells. Int J Nanomedicine **2,** 253, 2007.
31. Wall, M.E., Rachlin, A., Otey, C.A., and Loboa, E.G. Human adipose-derived adult stem cells upregulate palladin during osteogenesis and in response to cyclic tensile strain. Am J Physiol Cell Physiol **293,** C1532, 2007.
32. Bernacki, S.H., Wall, M.E., and Loboa, E.G. Isolation of human mesenchymal stem cells from bone and adipose tissue. Methods Cell Biol **86,** 257, 2008.
33. Wall, M.E., Bernacki, S.H., and Loboa, E.G. Effects of serial passaging on the adipogenic and osteogenic differentiation potential of adipose-derived human mesenchymal stem cells. Tissue Eng **13,** 1291, 2007.
34. Livak, K.J., and Schmittgen, T.D. Analysis of relative gene expression data using real-time quantitative PCR and the 2(-Delta Delta C(T)) Method. Methods **25,** 402, 2001.
35. Puetzer, J.L., Petitte, J.N., and Loboa, E.G. Comparative review of growth factors for induction of three-dimensional in vitro chondrogenesis in human mesenchymal stem cells isolated from bone marrow and adipose tissue. Tissue Eng Part B Rev **16,** 435, 2010.
36. Kim, Y.J., Kim, H.J., and Im, G.I. PTHrP promotes chondrogenesis and suppresses hypertrophy from both bone marrow-derived and adipose tissue-derived MSCs. Biochem Biophys Res Commun **373,** 104, 2008.
37. Tanaka, N., Ohno, S., Honda, K., Tanimoto, K., Doi, T., Ohno-Nakahara, M., Tafolla, E., Kapila, S., and Tanne, K. Cyclic mechanical strain regulates the PTHrP expression in

cultured chondrocytes via activation of the Ca^{2+} channel. J Dent Res **84,** 64, 2005.
38. de Crombrugghe, B., Lefebvre, V., and Nakashima, K. Regulatory mechanisms in the pathways of cartilage and bone formation. Curr Opin Cell Biol **13,** 721, 2001.
39. Goldring, M.B., Tsuchimochi, K., and Ijiri, K. The control of chondrogenesis. J Cell Biochem **97,** 33, 2006.
40. Yamaguchi, T., Chattopadhyay, N., Kifor, O., Ye, C., Vassilev, P.M., Sanders, J.L., and Brown, E.M. Expression of extracellular calcium-sensing receptor in human osteoblastic MG-63 cell line. Am J Physiol Cell Physiol **280,** C382, 2001.
41. Di Tomo, P., Pipino, C., Lanuti, P., Morabito, C., Pierdomenico, L., Sirolli, V., Bonomini, M., Miscia, S., Mariggio, M.A., Marchisio, M., Barboni, B., and Pandolfi, A. Calcium sensing receptor expression in ovine amniotic fluid mesenchymal stem cells and the potential role of R-568 during osteogenic differentiation. PLoS One **8,** e73816, 2013.
42. Martino, N.A., Lange-Consiglio, A., Cremonesi, F., Valentini, L., Caira, M., Guaricci, A.C., Ambruosi, B., Sciorsci, R.L., Lacalandra, G.M., Reshkin, S.J., and Dell'Aquila, M.E. Functional expression of the extracellular calcium sensing receptor (CaSR) in equine umbilical cord matrix size-sieved stem cells. PLoS One **6,** e17714, 2011.
43. Lam, B.S., Cunningham, C., and Adams, G.B. Pharmacologic modulation of the calcium-sensing receptor enhances hematopoietic stem cell lodgment in the adult bone marrow. Blood **117,** 1167, 2011.
44. Pipino, C., Di Tomo, P., Mandatori, D., Cianci, E., Lanuti, P., Cutrona, M.B., Penolazzi, L., Pierdomenico, L., Lambertini, E., Antonucci, I., Sirolli, V., Bonomini, M., Romano, M., Piva, R., Marchisio, M., and Pandolfi, A. Calcium sensing receptor activation by calcimimetic R-568 in human amniotic fluid mesenchymal stem cells: correlation with osteogenic differentiation. Stem Cells Dev **23,** 2959, 2014.
45. Martin, I., Miot, S., Barbero, A., Jakob, M., and Wendt, D. Osteochondral tissue engineering. J Biomech **40,** 750, 2007.
46. Lee, S.H., and Shin, H. Matrices and scaffolds for delivery of bioactive molecules in bone and cartilage tissue engineering. Adv Drug Deliv Rev **59,** 339, 2007.
47. Chen, F.H., Rousche, K.T., and Tuan, R.S. Technology insight: adult stem cells in cartilage regeneration and tissue engineering. Nat Clin Pract Rheumatol **2,** 373, 2006.
48. Kraus, K.H., and Kirker-Head, C. Mesenchymal stem cells and bone regeneration. Vet Surg **35,** 232, 2006.
49. Alexander, P.G., Gottardi, R., Lin, H., Lozito, T.P., and Tuan, R.S. Three-dimensional osteogenic and chondrogenic systems to model osteochondral physiology and degenerative joint diseases. Exp Biol Med (Maywood) **239,** 1080, 2014.
50. Keeney, M., and Pandit, A. The osteochondral junction and its repair via bi-phasic tissue engineering scaffolds. Tissue Eng Part B Rev **15,** 55, 2009.
51. Frenkel, S.R., Toolan, B., Menche, D., Pitman, M.I., and Pachence, J.M. Chondrocyte transplantation using a collagen bilayer matrix for cartilage repair. J Bone Joint Surg Br **79,** 831, 1997.
52. Sherwood, J.K., Riley, S.L., Palazzolo, R., Brown, S.C., Monkhouse, D.C., Coates, M., Griffith, L.G., Landeen, L.K., and Ratcliffe, A. A three-dimensional osteochondral composite scaffold for articular cartilage repair. Biomaterials **23,** 4739, 2002.
53. Lu, S., Lam, J., Trachtenberg, J.E., Lee, E.J., Seyednejad, H., van den Beucken, J.J., Tabata, Y., Wong, M.E., Jansen, J.A., Mikos, A.G., and Kasper, F.K. Dual growth factor delivery from bilayered, biodegradable hydrogel composites for spatially-guided osteochondral tissue repair. Biomaterials **35,** 8829, 2014.
54. Kolacna, L., Bakesova, J., Varga, F., Kostakova, E., Planka, L., Necas, A., Lukas, D., Amler, E., and Pelouch, V. Biochemical and biophysical aspects of collagen nanostructure in the extracellular matrix. Physiol Res **56(Suppl 1),** S51, 2007.

Address correspondence to:
Elizabeth G. Loboa, PhD
Joint Department of Biomedical Engineering
at University of North Carolina at Chapel Hill
North Carolina State University
911 Oval Drive
Engineering Building 111, Room 4208
Raleigh, NC 27695

E-mail: egloboa@ncsu.edu

Received: October 6, 2014
Accepted: May 21, 2015
Online Publication Date: July 10, 2015